Remote Sensing of Environment 114 (2010) 2436–2447

Contents lists available at ScienceDirect

Remote Sensing of Environment

journal homepage: www.elsevier.com/locate/rse

Multi-temporal monitoring of wetland water levels in the Florida Everglades using interferometric synthetic aperture radar (InSAR)

Sang-Hoon Hong [a,b,e,*,1], Shimon Wdowinski [a,1], Sang-Wan Kim [c], Joong-Sun Won [d]

[a] Division of Marine Geology and Geophysics, University of Miami, Miami, FL 33149-1098, USA
[b] Satellite Data Application Department, Korea Aerospace Research Institute (KARI), Daejeon, 305-333, Republic of Korea
[c] Department of Geoinformation Engineering, Sejong University, Seoul, 143-747, Republic of Korea
[d] Department of Earth System Sciences, Yonsei University, Seoul, 120-749, Republic of Korea
[e] Department of Civil and Environmental Engineering, Florida International University, 33174, USA

ARTICLE INFO

Article history:
Received 15 January 2010
Received in revised form 19 May 2010
Accepted 22 May 2010

Keywords:
Wetlands
Everglades
Interferometric synthetic aperture radar (InSAR)
Small baseline subset (SBAS)
Small temporal baseline subset (STBAS)
Absolute water levels

ABSTRACT

Interferometric synthetic aperture radar (InSAR) techniques can successfully detect phase variations related to the water level changes in wetlands and produce spatially detailed high-resolution maps of water level changes. Despite the vast details, the usefulness of the wetland InSAR observations is rather limited, because hydrologists and water resources managers need information on absolute water level values and not on relative water level changes. We present an InSAR technique called Small Temporal Baseline Subset (STBAS) for monitoring absolute water level time series using radar interferograms acquired successively over wetlands. The method uses stage (water level) observation for calibrating the relative InSAR observations and tying them to the stage's vertical datum. We tested the STBAS technique with two-year long Radarsat-1 data acquired during 2006–2008 over the Water Conservation Area 1 (WCA1) in the Everglades wetlands, south Florida (USA). The InSAR-derived water level data were calibrated using 13 stage stations located in the study area to generate 28 successive high spatial resolution maps (50 m pixel resolution) of absolute water levels. We evaluate the quality of the STBAS technique using a root mean square error (RMSE) criterion of the difference between InSAR observations and stage measurements. The average RMSE is 6.6 cm, which provides an uncertainty estimation of the STBAS technique to monitor absolute water levels. About half of the uncertainties are attributed to the accuracy of the InSAR technique to detect relative water levels. The other half reflects uncertainties derived from tying the relative levels to the stage stations' datum.

1. Introduction

Wetlands are zone with excess water, where nutrient cycling and the sun's energy meet to produce a very productive ecosystem (Mitsch & Gosselink, 2007; Rivera, 2005). They encompass a wide variety of aquatic habitats, home for a wide variety of plant and animal species. Wetlands also have a valuable economical importance, as they prevent flooding, filter nutrients and pollutants from fresh water used by humans, and provide aquatic habitats for outdoor recreation. Due to severe population growth, land proclamation, and urbanization, many wetlands are under severe environmental stress. However, the increasing recognition of wetland importance has led to restoration activities in a few regions. As these ecosystems are water dependent, hydrological monitoring of the wetlands is critical for management and restoration. Typically, hydraulic monitoring of wetlands is conducted by stage (water level) stations providing good temporal resolution at a finite number of observation points. However, these measurements have limited capability to detect spatial patterns, because stage stations are typically distributed several, or even tens of kilometers, from one another. Furthermore, in some rural areas it is difficult to get stage record even from a single site, resulting in a very limited knowledge of the wetland hydrological conditions.

Significant spatial resolution improvements were achieved by interferometric synthetic aperture radar (InSAR) observations, which measure water level changes over wide areas with 5–100 m pixel resolution and several centimeters vertical accuracy (Alsdorf et al., 2000; Wdowinski et al., 2004). The wetland InSAR technique works where vegetation emerges above the water surface due to the "double bounce" effect, in which the radar pulse is backscattered twice from the water surface and vegetation (Richards et al., 1987). InSAR observations were successfully used to study wetland hydrology in the Everglades (Hong et al., 2010; Wdowinski et al., 2004, 2008), Louisiana (Kim et al., 2008; Lu & Kwoun, 2008; Lu et al., 2005) and the Sian Ka'an in Yucatan (Gondwe et al., 2010). However despite the vast spatial details, the usefulness of the wetland InSAR observations remained limited, because (1) hydrologists and water resources managers need information on absolute water

* Corresponding author. Department of Civil and Environmental Engineering, Florida International University, 33174, USA. Tel.: +82 42 870 3962; fax: +82 42 860 2605.
E-mail addresses: shong@kari.re.kr (S.-H. Hong), shimonw@rsmas.miami.edu (S. Wdowinski), swkim@sejong.ac.kr (S.-W. Kim), jswon@yonsei.ac.kr (J.-S. Won).
[1] Tel.: +1 305 421 4909; fax: +1 305 421 4632.

0034-4257/$ – see front matter © 2010 Elsevier Inc. All rights reserved.
doi:10.1016/j.rse.2010.05.019

level values and not on relative water level changes, as wetland surface flow is driven mainly by gravitational potential induced by lateral water levels differences; (2) the static nature of InSAR observations. An interferogram detects water level changes between two snapshots in time, which are the SAR data acquisition times, and hence the interferogram has limited capability describing the dynamic nature of wetland surface flow; and (3) the InSAR technique is computational intensive, involves a lot of expert processing on appropriate image pairs that are still largely only opportunistic for most regions of the world.

A significant progress in InSAR technology was the development of persistent scatterer InSAR (PSI) (Ferretti et al., 2000, 2001) and small baseline subset (SBAS) techniques (Berardino et al., 2002; Lanari et al., 2004), which use a large number of SAR observations to monitor displacement time series using successive InSAR observations. In this study we adopt the same multi-temporal approach developed by the PSI and SBAS methods to obtain InSAR time series of wetland surface water level changes. Furthermore, we integrate the space-based observations with ground-based stage observations to tie the InSAR measurements the stage datum and obtain high-resolution maps of 'absolute' surface water levels. Our methodology follows the SBAS technique, but with some modifications. The major modification is the interferometric pair selection criterion. The SBAS technique uses small geometric baselines criterion, whereas we use small temporal baseline criterion, because interferometric coherence over wetlands is maintained over short time periods (Hong & Won, 2006; Kim et al., submitted for publication). Hence, we call our modified method Small Temporal Baseline Subset analysis (STBAS). We test the new technique by applying it to a section of the south Florida's Everglades using a two-year long Radarsat-1 observations. The goal of this study is to reconstruct absolute water level time series instead of previous approaches calculating only relative water level changes, or absolute level during a single time period.

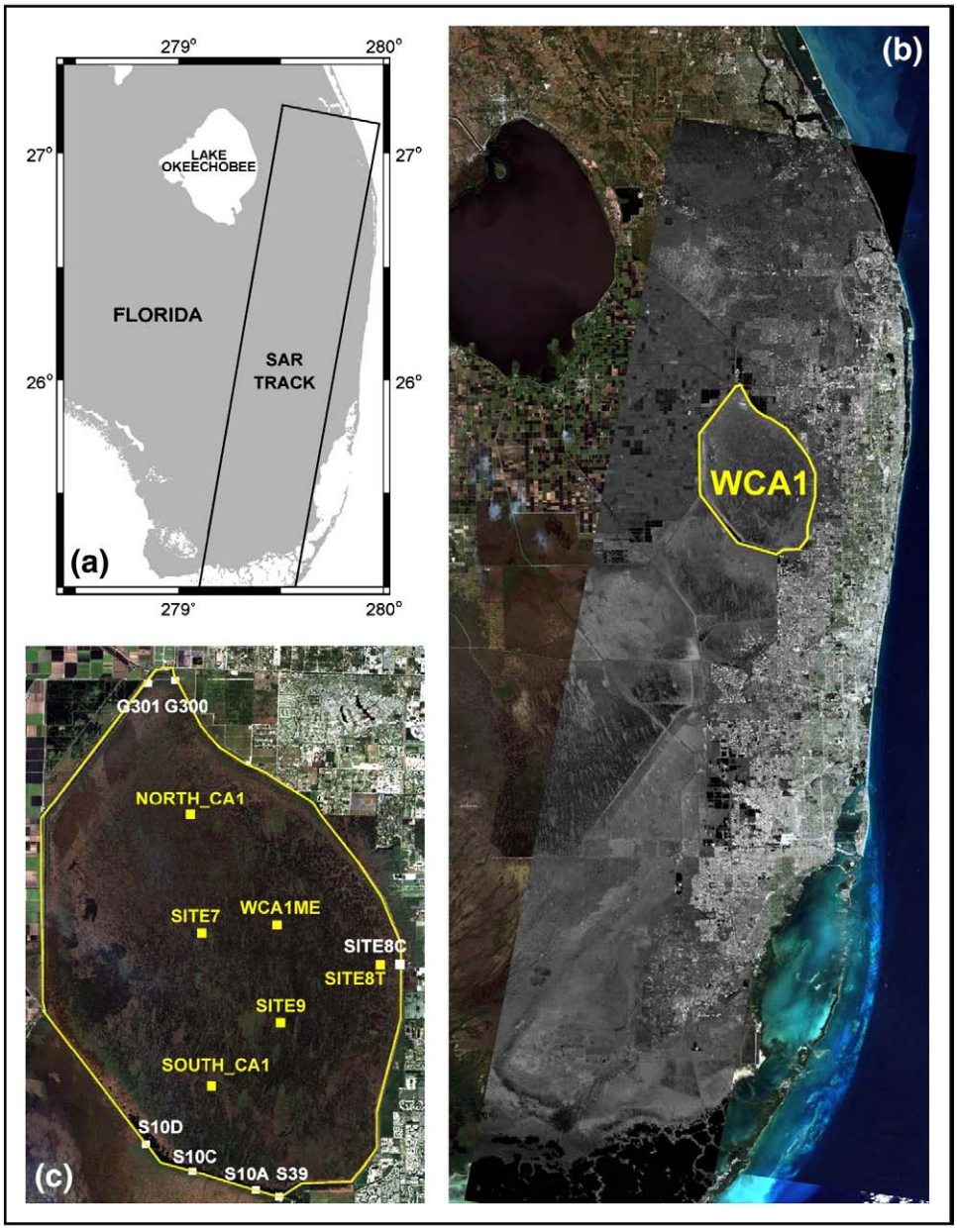

Fig. 1. (a) Location map showing the SAR track used in this study, (b) composite satellite image showing the study area, WCA1. The SAR track shows the average amplitude strip map (RADARSAT data © Canadian Space Agency/Agence spatial canadienne 2002. Processed by CSTARS and distributed by RADARSAT International) overlies Landsat ETM + optical image, and (c) satellite image showing the location of stage stations in the WCA1 area. White squares mark station location along the peripheral canals and yellow squares mark location of stations located within the interior of the area.

2. Study area

Our study area is Water Conservation Area 1 (WCA1), which is located in the northern section of the Everglades wetlands, south Florida, approximately 30 km southeast of Lake Okeechobee (Fig. 1a,b). It is an independent water storage unit of size 85 km^2, surrounded by peripheral canals and levees, and managed by the South Florida Water Management District (SFWMD). We chose to demonstrate our new multi-temporal technique in this area, because the hydrodynamics of this area is relatively simple compared with any other open wetland areas. Furthermore the area is monitored by 13 stage stations (Fig. 1c), which provide an excellent data set for calibration, validation and quality assessment of the STBAS technique.

WCA1 is a remnant of a large wetland system that occupied south Florida until a century ago. This area also serves as a wildlife refuge providing natural wetland conditions for a wide variety of plants and animals. It is also a part of a water reservoir system supplying water for the large human population (>5 million) living along the eastern coast of south Florida. In order to sustain the natural ecosystem, water levels are kept there at relatively high levels. The overall flow pattern in WCA1 is a north–south flow; water is charged from the north and is released in the south into Water Conservation Area 2A (WCA2A). The typical flow pattern in the area is radial from the peripheral canals into the wetland interior, or from the area interior to the canals. Such flow occurs during the wet season (May–October) when water levels are high. The dry season (November–April) is characterized relatively flat water conditions.

3. Data

This study relies on two data sets, one is space-based SAR observations and the other is ground-based stage data. We used 29 Radarsat-1 C-band fine beam (mode 5) SAR observations with HH polarization acquired over south Florida between Jan 29, 2006 and Jan 19, 2008. Radarsat-1 has been operated with a C-band (5.3 GHz frequency and 5.6 cm wavelength) by Canadian Spacing Agency (CSA) since 1995 till present. The characteristics of the Radarsat-1 SAR data are described in Table 1. The temporal baselines, which are the time span between two acquisitions of SAR data, of interferometric pairs are 24 days except two pairs (their temporal baselines are 48 days). The range of their absolute geometric baselines, which are separation between two satellite orbits, extends from 64 m to 1367 m (Fig. 2). The detail parameters of interferometric pairs are shown in Table 2.

The InSAR data were calibrated with daily average stage data monitored by 13 stage stations located within WCA1. The locations of stage stations over WCA1 are displayed in Fig. 1. There are two types of stage stations in WCA1. The first type is peripheral canal station located along the levees and the second type is the marsh station located in the interior WCA1. All stations are part of a large network of stations located throughout the Everglades and are operated by SFWMD, U. S. Geological Survey (USGS), Everglades National Park (ENP), and Big Cypress National Preserve (BCNP). We obtained the data from the Everglades Depth Estimation Network (EDEN) archive (http://sofia.usgs.gov/eden/stationlist.php), which provides daily average levels above NAVD88 and NGVD29 datum. Stage stations with NGVD29 datum were converted to NAVD88 datum. The information of stage stations is summarized in Table 3.

The stage data provide an excellent dataset for ground truthing. However, it needs a careful editing, because Lin and Gregg (1988) pointed out that some stage stations located near hydraulic structures, such as gates, are affected by the flow dynamics and can provide

Table 1
Radarsat-1 synthetic aperture radar data characteristics.

Parameter	Radarsat-1
Carrier frequency	5.300 GHz
Wavelength	5.6 cm
Polarization	HH
Repeat period	24 days
Beam mode	Fine beam 5 (F5)
Flight direction	Descending
Incidence angle	46.50 °
Pulse repetition frequency	1301.95 Hz
ADC sampling rate	32.32 MHz
Azimuth pixel spacing	5.16 m
Range pixel spacing	4.64 m

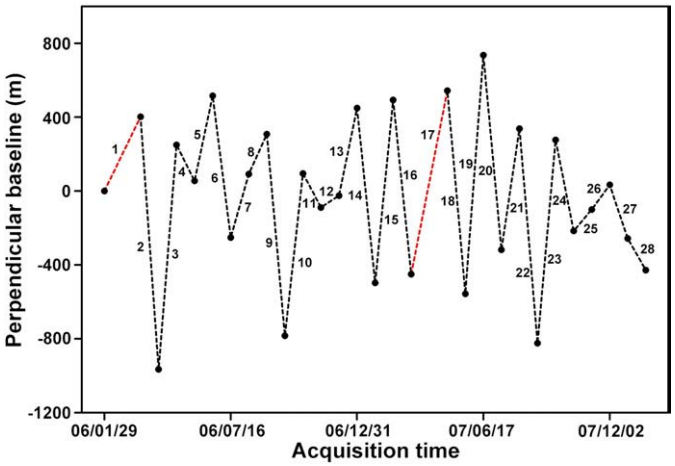

Fig. 2. Perpendicular baseline information presented with respect to the first SAR acquisition. Black dash lines mark 24-day time span between successive (temporal baselines) acquisitions and red dash lines mark 48-day temporal baselines. The range of geometrical perpendicular baselines varies from 64 m to 1367 m. The number mark the interferometric pair as listed in Table 2.

Table 2
List of Radarsat-1 C-band SAR interferometric pairs.

No	SAR image		$B_\perp$ [a]	B_{temp} [b]	γ_{mean} [c]
	Master	Slave			
1	06/01/29	06/03/18	402 m	48 days	0.17
2	06/03/18	06/04/11	1367 m	24 days	0.17
3	06/04/11	06/05/05	1215 m	24 days	0.15
4	06/05/05	06/05/29	195 m	24 days	0.19
5	06/05/29	06/06/22	461 m	24 days	0.19
6	06/06/22	06/07/16	768 m	24 days	0.15
7	06/07/16	06/08/09	344 m	24 days	0.20
8	06/08/09	06/09/02	216 m	24 days	0.16
9	06/09/02	06/09/26	1092 m	24 days	0.18
10	06/09/26	06/10/20	879 m	24 days	0.17
11	06/10/20	06/11/13	184 m	24 days	0.20
12	06/11/13	06/12/07	64 m	24 days	0.18
13	06/12/07	06/12/31	474 m	24 days	0.18
14	06/12/31	07/01/24	946 m	24 days	0.20
15	07/01/24	07/02/17	990 m	24 days	0.20
16	07/02/17	07/03/13	943 m	24 days	0.15
17	07/03/13	07/04/30	993 m	48 days	0.15
18	07/04/30	07/05/24	1009 m	24 days	0.21
19	07/05/24	07/06/17	1292 m	24 days	0.18
20	07/06/17	07/07/11	1054 m	24 days	0.17
21	07/07/11	07/08/04	656 m	24 days	0.15
22	07/08/04	07/08/28	1162 m	24 days	0.17
23	07/08/28	07/09/21	1101 m	24 days	0.21
24	07/09/21	07/10/15	493 m	24 days	0.17
25	07/10/15	07/11/08	116 m	24 days	0.20
26	07/11/08	07/12/02	134 m	24 days	0.18
27	07/12/02	07/12/26	291 m	24 days	0.21
28	07/12/26	08/01/19	171 m	24 days	0.18

[a] $B_\perp$ — absolute perpendicular baseline.
[b] B_{temp} — temporal baseline.
[c] γ_{mean} — an average coherence.

Table 3
Type, location and datum of WCA1 stage stations.

Station	Type	Latitude	Longitude	Datum	Agency	Cp[a] (ft)
SITE8T	Marsh	26°29′59″	−80°14′05″	NGVD29	USGS	−1.47
SITE8C	Canal structure	26°30′01″	−80°13′21″	NGVD29	USGS	−1.47
S39_H	Canal structure	26°21′21″	−80°17′53″	NAVD88	SFWMD	–
S10A_H	Canal structure	26°21′36″	−80°18′45″	NGVD29	USGS	−1.49
S10C_H	Canal structure	26°22′18″	−80°21′09″	NGVD29	USGS	−1.47
S10D_H	Canal structure	26°23′19″	−80°22′54″	NGVD29	USGS	−1.46
G301_T	Canal structure	26°40′31″	−80°22′49″	NAVD88	SFWMD	–
G300_T	Canal structure	26°40′37″	−80°21′48″	NAVD88	SFWMD	–
NORTH_CA1	Marsh	26°35′38″	−80°21′13″	NAVD88	USGS	–
SITE7	Marsh	26°31′11″	−80°20′49″	NGVD29	USGS	−1.46
WCA1ME	Marsh	26°30′39″	−80°18′36″	NAVD88	SFWMD	–
SITE9	Marsh	26°27′51″	−80°17′49″	NGVD29	USGS	−1.48
SOUTH_CA1	Marsh	26°25′29″	−80°20′26″	NAVD88	USGS	–

[a] Cp is reported vertical conversion parameter at gauge from NGVD29 to NAVD88 datum.

inaccurate stage values. In order to evaluate the data quality, we plotted water levels of the canal and interior stations for the 29 collected SAR acquisition dates as shown in Fig. 3. The water levels in canal stations show similar height, but spanning over a wide range. High water levels occur in the wet season and low in the dry season. The interior stations show a different pattern. During high water condition, the stations show flat water level. During the dry and some of the wet season, the stations show variable height, basically a southward decrease, which is consistent with the overall N–S flow pattern. Because of the high flow rate in the canals, water levels along the canals cannot deviate much. As indicated by Lin and Gregg (1988), deviation occurs locally due to an operation of a hydraulic structure. We detected deviations in the stages (especially S39_H and G300_T), and edited these local flow-induced deviations by assuming flat canal level conditions (dashed lines in Fig. 3).

4. Methodology

Our STBAS methodology for obtaining InSAR time series of absolute water levels relies on both SAR and stage data. The SAR data is used to calculate high-resolution maps of water level changes and the stage data is used for calibrating the InSAR data, tying the relative observations to the stage's datum, and verifying the results. Our STBAS methodology is based on the SBAS algorithm, but involves additional steps that are needed for the calibration of the InSAR observations with the stage data. It consists of the five steps. The first three steps are conducted at the independent interferogram level and the last two steps connect all the information in order to estimate time series. The five steps are: 1) selection of small temporal baseline interferometric pairs, 2) interferogram generation of each pair including phase unwrapping, 3) calibration of water level changes with stage water level data, 4) estimation of relative water level time series from the calibrated water level changes using Singular Value Decomposition (SVD) inversion (Press et al., 2002), and 5) estimation of absolute water levels time series by tying the relative series to reference water levels. The algorithm includes two calibration steps, where stage data are used to tie the relative InSAR observations. The first calibration is conducted in step 3 for each interferogram. The second calibration is conducted in step 5, where the entire InSAR time series is tied to the stage datum. A visual representation of the algorithm is illustrated by a flow chart in Fig. 4. In the rest of this section we present the five steps in both general terms that can be applied to any SAR dataset and with the specific example of WCA1.

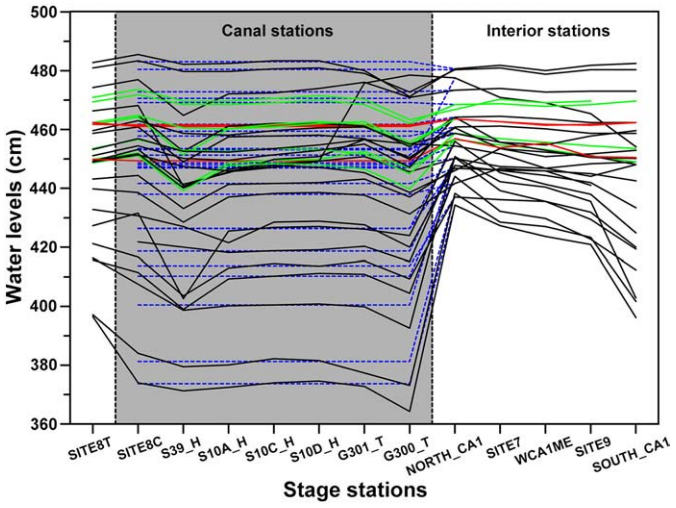

Fig. 3. Reported (black) and corrected (blue) stage water levels during the SAR data acquisitions. The canal stations are listed in a clockwise loop and the interior stations along the N–S transect. The canal water levels near hydrological structures are often distributed by dynamic flow Kim et al. (submitted for publication) and, hence, were corrected according to the rest of the canal stations (blue dashed lines). The red lines mark nearly flat water conditions used as reference elevations in step 5.

Step 1 — *pair selection*: our analysis relies on repeat pass SAR data acquisition that can process to produce coherent interferograms. As indicated above, short temporal baseline is the key for obtaining best interferometric coherence over wetlands. Thus, in this step we select pairs with shortest temporal baseline regardless of the geometrical baseline.

WCA1 example: we selected only minimum temporal baselines of the interferometric pairs. In our RADARSAT-1 dataset, most temporal baselines are of 24 days except two pairs with 48 days temporal baselines (Fig. 2 and Table 2).

Step 2 — *interferogram calculation*: in this step we calculate interferograms for each selected pair including removal of the flat earth phase and topography phase and unwrapping processing. The orbit inaccuracy is compensated using estimation of refined baseline from interferogram fringe spectrum with full swath data. A careful examination of unwrapped phase is needed because phase discontinuities can result from low coherence.

WCA1 example: we processed all selected pairs using the ROI_PAC software package (Buckley et al., 2000). We generated 28 coherent interferograms including phase unwrapping and topographic phase removal based on the SRTM-1 digital elevation model (DEM). In order to improve fringe visibility, adaptive radar interferogram filter and multi-looking processes were applied (Goldstein & Werner, 1998). The spatial filtering and multi-looking increased the signal to noise ratio but reduced the spatial resolution as phase is averaged over several pixels. The spatial resolution of the filtered interferograms varies from 7 m to about 50 m, because the filtering procedure determines dynamically the averaging window according to the noise

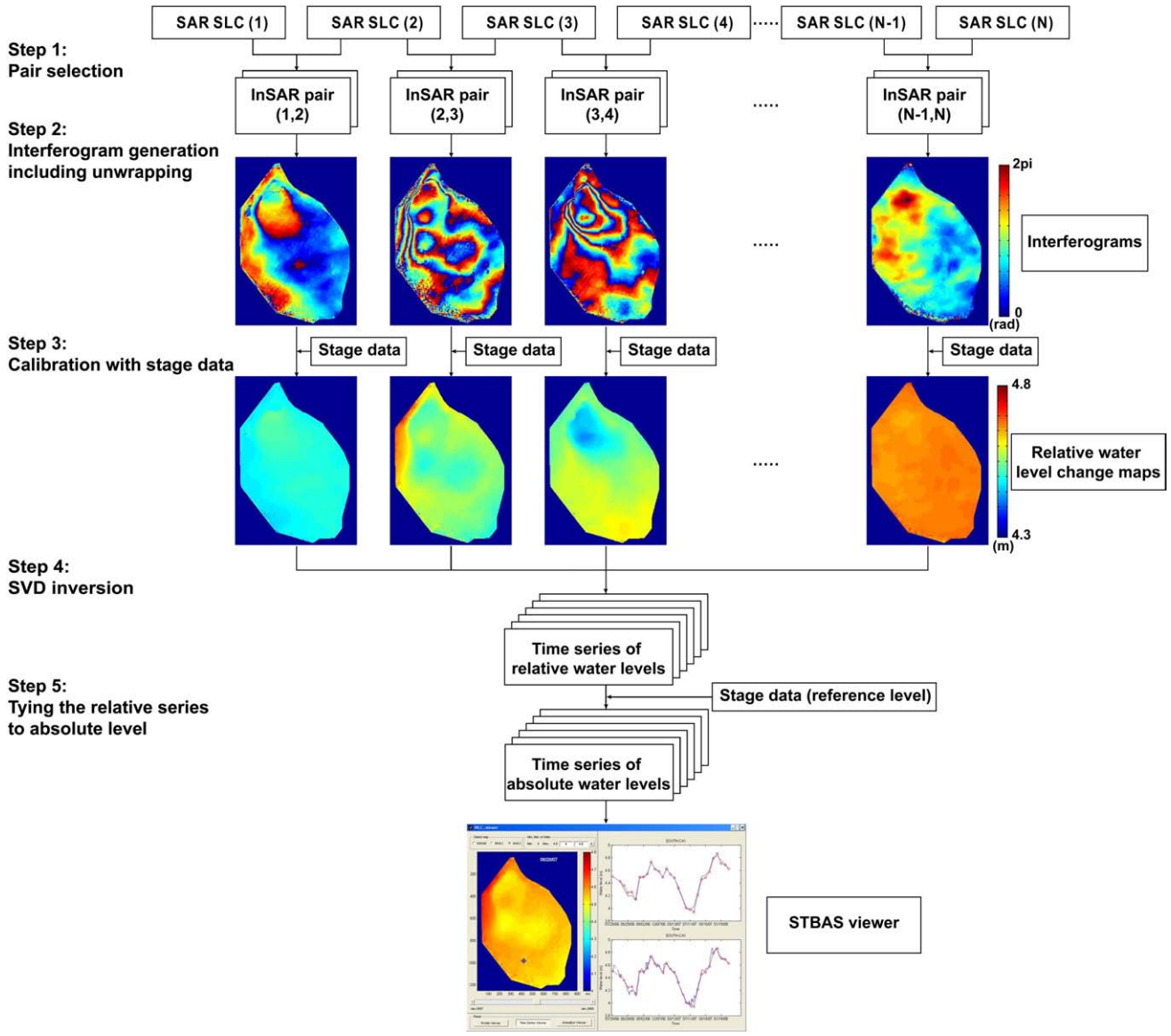

Fig. 4. Flowchart of STBAS technique describing the algorithm for monitoring absolute water level time series.

level. Before unwrapping interferometric phases, the phases outside barriers was masked out in order to overcome the presence of phase discontinuities. Unwrapped interferometric phases were transformed from radar to geographic coordinate system (geodetic projection on WGS 84 datum). The final product of this step is a set of unwrapped filtered interferograms showing phase changes due to water level changes (Fig. 5).

Step 3 — *calibration with stage data*: the InSAR observations are in phase (radian) describing relative surface displacement in both space and time. They represent water level changes between two acquisition dates with respect to a reference point. In solid earth deformation studies, such as earthquake-induced deformation, undeformed location point in a far field area is typically chosen as a reference point. However in wetlands, especially in managed wetlands, water levels can be discontinuous across barriers such as levees, and hence a far field point located beyond a barrier cannot be used as reference. Instead we define an arbitrary reference height, which is calibrated using stage data. A detailed description of the conversion of the phase data to water level changes (in centimeters) and the actual calibration procedure is provided by Wdowinski et al. (2008) and the Electronic Supplement 1.

*WCA*1 *example*: the first part of the calibration procedure, the conversion of the phase data into water level changes (Eq. ES-1) is straightforward. However, the actual comparison between the InSAR and stage observations requires a careful supervision, because (i) most of the peripheral canal stage stations are located in low coherence areas, suggesting poor phase and, consequently, poor estimation of water level change at the actual station locations (Fig. 6), (ii) some InSAR and/or stage data values may represent an unreasonable value (outliers) and should be removed, and (iii) some of the stage data are used for verification and should not be included in the calibration stage.

In order to overcome the low coherence problem of the peripheral canal stations, we introduced a virtual station analysis, in which we selected locations with higher coherence around original canal stations, and evaluated height differences between InSAR and stage observations at the virtual station locations. Detailed description of the virtual stage station analysis is provided in the Electronic Supplement 2. The implementation of this analysis significantly improves the quality of the STBAS algorithm. The outlier detection and the calibration versus validation subset selection were conducted as part of the calibration between the InSAR and stage data (Fig. 7). The calibration plots show good agreement between InSAR and stage data in 22 out of 28 interferometric pairs. Six calibration plots (Fig. 7 (3), (17), (18), (19), (20) and (26)) show poor agreement between the InSAR and stage data. In three of the plots (Fig. 7 (3), (17), and

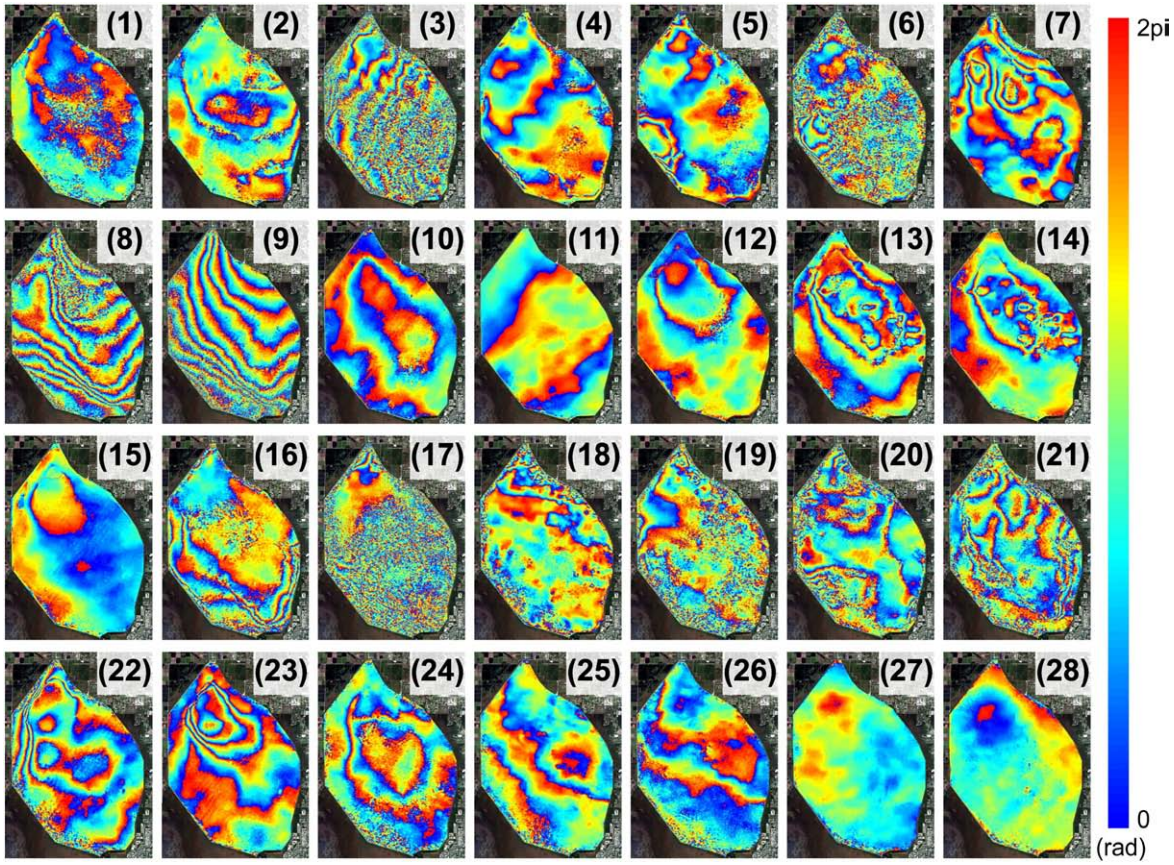

Fig. 5. Interferogram time series of the study area. Although the interferograms are unwrapped, fringes are displayed with a 0–2π scale, in order to recognize surface change patterns. Number in each plot corresponds to the interferometric pair number listed in Table 2.

(19)), the poor agreement reflects a lower quality of the InSAR data due to the overall low coherence of the interferograms occurring at low water levels at the end of the dry season (Fig. 5). In the other three plots, the low agreement arises from a subset of stations located in low coherence areas, mainly in the southern section of WCA1 (Fig. 6).

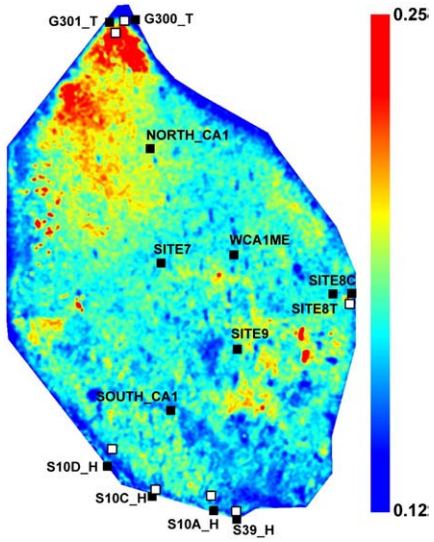

Fig. 6. Stage station location (black squares) overlying a map showing average coherence over the study area. The low coherence occurs along the peripheral canals in open water or sparse vegetation areas. White box squares mark selected virtual stage stations located in higher coherence area near original peripheral stage stations. The details of the virtual station analysis are provided in the Electronic Supplement.

The final product of this calibration step is a set of water level change maps time series with calibrated offset (Fig. 8).

Step 4 — *estimation of relative water level time series*: here we combine all the calculated observations from each water level change map into a continuous set of observations, a time series of relative water level changes. The estimation of water level in time series is accomplished by a SVD inversion. Accordingly, an estimate of the water level time series is achieved for each coherent pixel. However, the calculated result also contains information of the unwanted atmospheric artifacts or other decorrelation effects as well as water level variations. In SBAS application, atmospheric artifact effects are removed by a filtering procedure derived from the PSI approach (Berardino et al., 2002; Lanari et al., 2004). The assumption used by SBAS is that the atmospheric effects are totally decorrelated with the deformation changes in time. However, the atmospheric contribution phase removal approach is not possible in the wetland application, because water level changes fluctuate daily and with variable lateral scales. Thus, some level of atmospheric noise remains in the water level time series.

*WCA*1 *example*: we performed a SVD inversion to combine all the observations from each water level change maps into a time series of relative water level changes. The final product of this step is a time series of relative water level changes.

Step 5 – *estimation of absolute water level time series*: the absolute water level time series is accomplished by tying the relative water level time series (step 4) to reference water level conditions. The relative time series produced in the previous step describes water level changes for each pixel. However, the absolute water level elevation is known only at finite locations where stage data are available. In order to expand this knowledge to all pixels, we need to define a reference level, preferably during flat water level conditions,

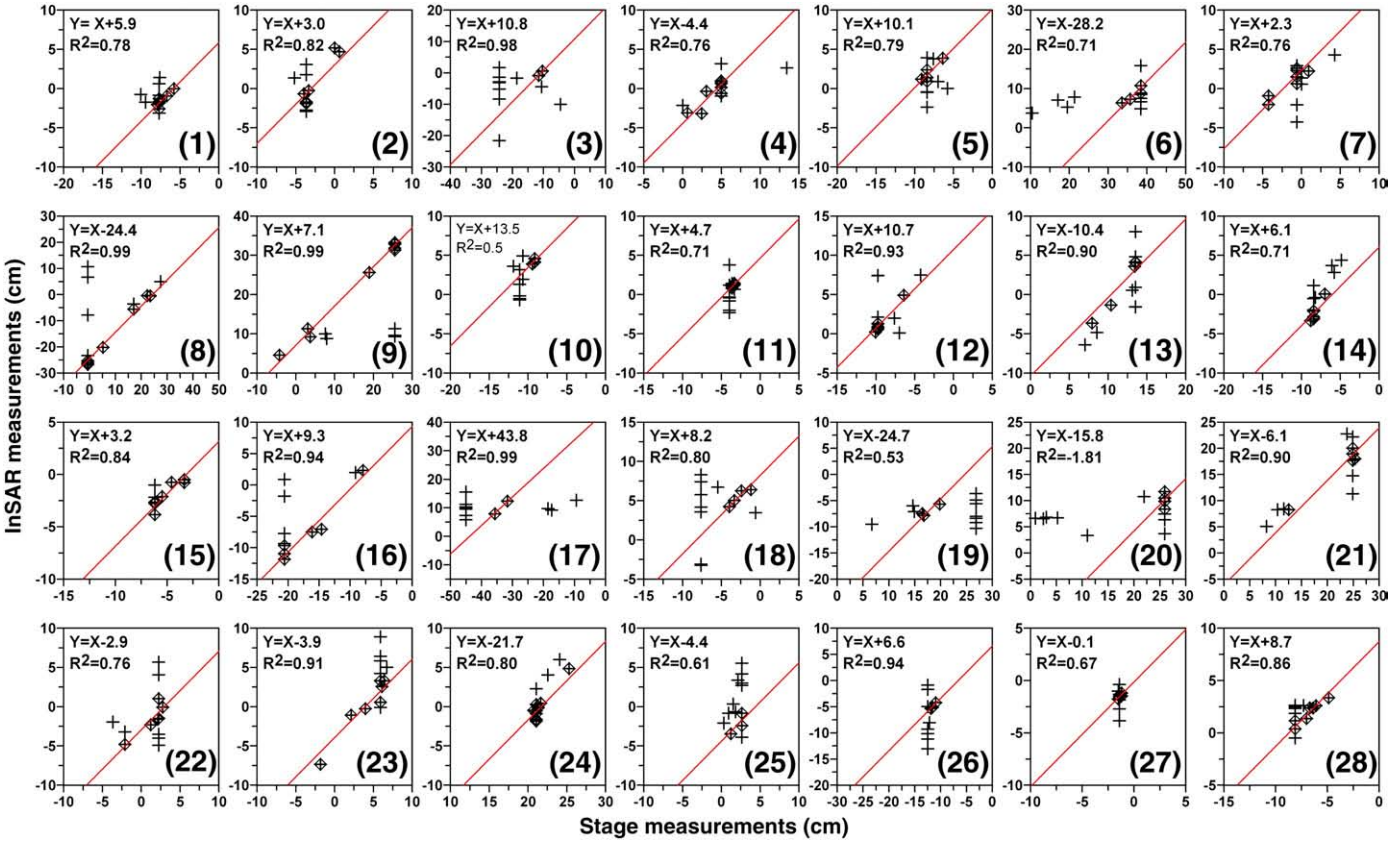

Fig. 7. Calibration plots for estimating the offsets between InSAR and stage station observations. Most of the calibrations show good agreement. Number in each plot corresponds to the interferometric pair number listed in Table 2. The symbol "+" marks outliers that are omitted from the calibration offset calculations.

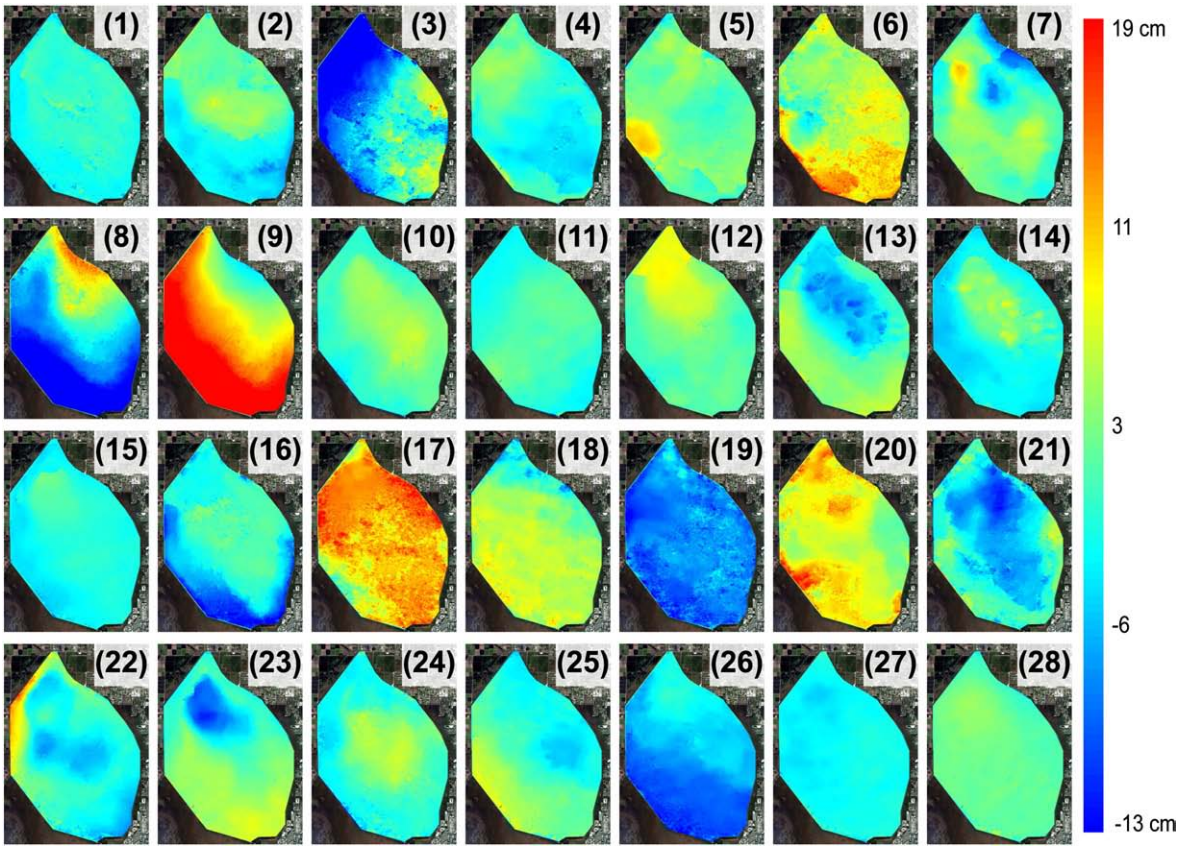

Fig. 8. Calibrated water level change time series maps over the study area. Number in each plot corresponds to the interferometric pair number listed in Table 2.

Table 4
Uncertainty analysis based on RMSE calculations (in centimeters) between the InSAR and stage measurements. The bold styled values are used stage stations in calibration step 5.

		Canal stations							Interior stations					
Test ID.	Site8T	Site8C	S39_H	S10A_H	S10C_H	S10D_H	G301_T	G300_T	North_CA1	Site7	WCA1ME	Site9	South_CA1	Average
1	**4.5**	**8.5**	**7.2**	**5.9**	6.4	**3.9**	**7.7**	8.0	**10.0**	7.0	7.5	**6.8**	**3.0**	6.6
2	**4.5**	**8.5**	**7.2**	**5.9**	6.4	**3.9**	**7.7**	8.0	**10.0**	**7.0**	7.5	**6.8**	**3.0**	6.6
3	**4.5**	**8.5**	**7.2**	**5.9**	**6.7**	**3.9**	**7.7**	7.9	**10.0**	7.0	7.5	**6.8**	**3.0**	6.7
4	**4.5**	**8.5**	**7.2**	**5.9**	**6.7**	**3.9**	8.2	**8.2**	**10.0**	7.1	7.5	**6.8**	**3.0**	6.7
5	**4.5**	**8.5**	**7.2**	**5.9**	**6.7**	**3.9**	**7.7**	**8.2**	**10.0**	**7.5**	**7.7**	**6.8**	**3.0**	6.7
6	**4.5**	**8.5**	**7.2**	**5.9**	**6.7**	**3.9**	**7.7**	**8.2**	**10.0**	8.2	**7.7**	6.5	**3.0**	6.7
7	**4.5**	**8.5**	**7.2**	8.3	**6.7**	**3.9**	**7.7**	8.0	**10.0**	7.1	7.4	**6.8**	**3.0**	6.8
8	5.1	**8.5**	**7.2**	8.3	6.6	**3.9**	**7.7**	**8.2**	**10.0**	**7.5**	**7.7**	**6.8**	**3.0**	6.9
9	**4.5**	**8.5**	**7.2**	8.2	6.4	**3.9**	**7.7**	**8.2**	**10.0**	7.0	9.2	7.7	**3.0**	7.0
10	**4.5**	**8.5**	**7.2**	8.5	6.5	**3.9**	**7.7**	**8.2**	12.7	**7.5**	**7.7**	**6.8**	**3.0**	7.1
11	**4.5**	**8.5**	**7.2**	8.6	6.5	**3.9**	**7.7**	**8.2**	12.5	**7.5**	8.1	6.8	**3.0**	7.1
12	**4.5**	**8.5**	13.1	**5.9**	6.4	**3.9**	**7.7**	**8.2**	**10.0**	**7.5**	8.1	7.1	**3.0**	7.2
13	**4.5**	**8.5**	**7.2**	9.8	6.6	**3.9**	**7.7**	8.0	**10.0**	7.0	7.4	**6.8**	7.4	7.3
14	5.1	**8.5**	**7.2**	7.8	8.1	11.4	**7.7**	7.9	**10.0**	7.5	7.7	**6.8**	**3.0**	7.6
Average	4.6	8.5	7.6	7.2	6.7	4.4	7.7	8.1	10.4	7.3	7.8	6.9	3.3	6.9

that ties all individual water level series in each pixel to the same absolute reference elevation.

WCA1 example: in our study area, WCA1, flat water conditions occur in the beginning of dry season, typically during December–January. Towards the end of the dry season, some sections of the wetlands dry up. During the wet season, rain and human-induced flow cause lateral elevation change of 30–80 cm (Fig. 3). However lateral elevation variations during the December–January are of 0–10 cm, allowing us to use these almost flat surfaces as our reference elevation. We used multiple calibration reference levels (e.g. red lines in Fig. 3 at an interval of a year in our study) in order to minimize error propagation from one acquisition date to the next. Large error occurs during low coherence conditions mainly towards the end of the dry season (March–May). We evaluated the fit quality between the InSAR and stage observations using RMSE calculations in 14 different tests (Table 4). In each test, we chose a different arbitrary subset of stations for the calibration (bold fonts in Table 4) and the difference between the InSAR and stage observations in all the stations for the RMSE calculations. The best results of our uncertainty analysis are shown as maps of absolute water levels (Fig. 9).

5. Results

We successfully applied the STBAS algorithm to estimate absolute water levels time series in WCA1. At the end of this process, we obtained two invaluable products (1) high spatial resolution maps of

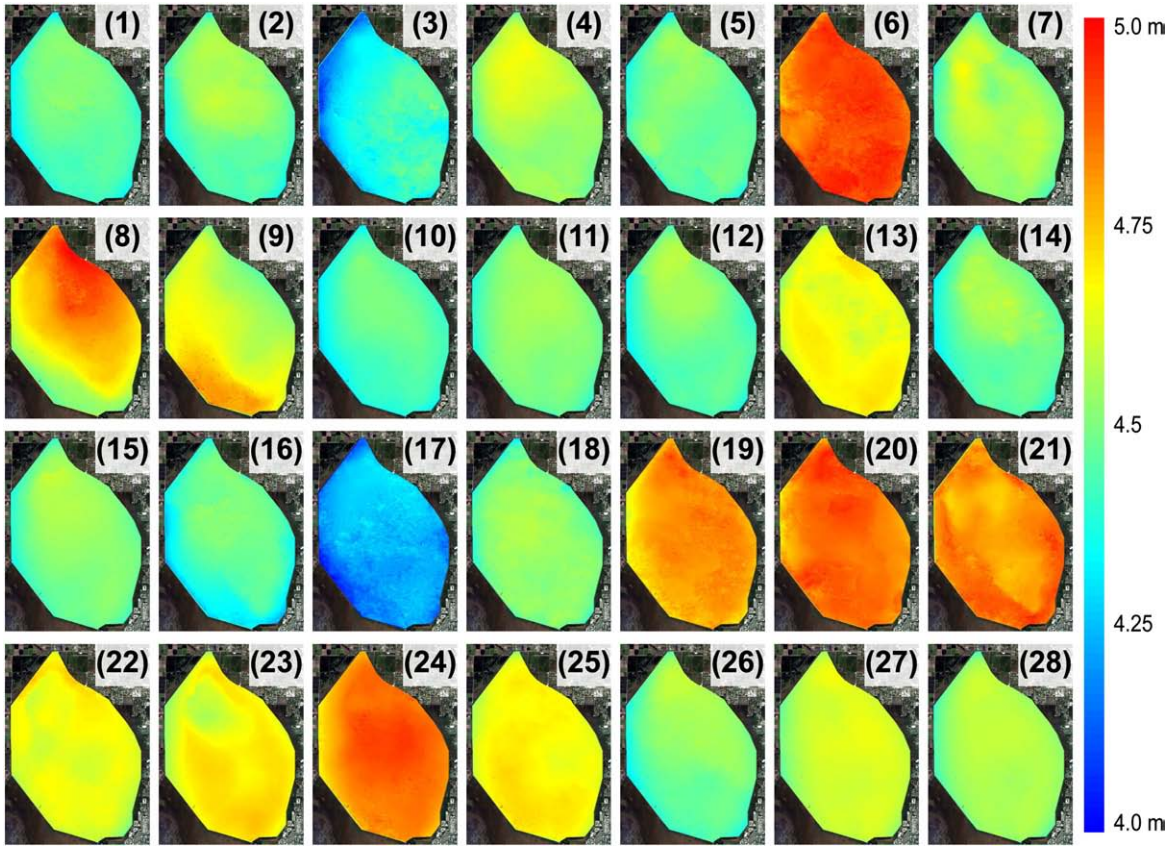

Fig. 9. Calibrated absolute water level time series maps over the study area. Notice the change in the scale (4–5 m) with respect to that of water level changes (32 cm in Fig. 7). Number in each plot corresponds to the interferometric pair number listed in Table 2.

absolute water levels and (2) absolute water level time series for almost every pixel. The calibrated absolute water level map time series are of high spatial resolution (50 m) and about 6–7 cm vertical accuracy (Table 4). The second product, water level time series, contains 28 data points over a two-year period with time spacing of 24 days except two missing acquisition (Fig. 10). Although the temporal resolution obtained by our analysis is fairly poor, it is calculated for almost every pixel (50 m resolution). Hence, it provides very useful information especially for areas located far from the stage stations.

The measured water level time series are in a good agreement with the stage data. We evaluated the quality of our results using RMSE analysis showing that the overall fit between the InSAR and stage data is good (Fig. 10), with average misfit level of 6–7 cm (Table 4). RMSEs in all stage stations (except NORTH_CA1 station) are below 10 cm. The results of the uncertainty analysis as referred in Section 4 are shown in Table 4. The average RMSE of all test sets is 6.9 cm, and the best result is 6.6 cm. The best performing stage station is the SOUTH_CA1 showing 3.3 cm average RMSE and the worst performing station is the NORTH_CA1 station whose RMSE is 10.8 cm. The current 7 cm RMSE level was achieved thanks to the virtual stage station procedure (Electronic Supplement). Before we implemented this procedure, the RMSE was in the 16–18 cm level.

In order to allow easy access to the InSAR-based time series observations, we developed a STBAS tool with interactive graphical user interface (GUI) for displaying water level maps, time series and water level points. It provides efficient visualization of water level information for all pixels in the wetland. It is a very useful tool for management purposes as well as research.

6. Discussion

One of the main advantages of the STBAS technique is its capability to transform the relative InSAR water level change observations to absolute water levels. Wetland InSAR observations provide high spatial resolution (50 m pixel) maps of surface water level changes occurring between the two data acquisition dates (Alsdorf et al., 2000; Wdowinski et al., 2004). Such maps can detect flow discontinuities, provide insight on surface flow patterns, and can constrain quantitative flow models (Wdowinski et al., 2006). Unfortunately, most hydrologists are not used to think in terms of relative measurements (water level changes) and, hence, do not make much use of the InSAR observations. However, they are very interested in high-resolution maps of absolute water levels. Thus, the transition from relative to absolute levels is crucial for enabling the space-based observations to end-users, such as hydrologists and water resources managers.

The STBAS method is based on a similar InSAR time series technique, SBAS (Berardino et al., 2002; Lanari et al., 2004), but also different. The main difference is the subset selection. The SBAS uses small geometrical baseline subsets, whereas the STBAS uses small temporal baseline subsets. However, the STBAS method is limited only by critical geometrical baselines, because interferograms with too long baselines (greater than critical baselines) are incoherent. The STBAS method is more suitable for the wetland application, because small temporal baselines are critical for maintaining coherence over wetlands. The method can also be useful in other rapid changing surfaces such like ice sheet (Hong & Won, 2006).

The most reliable way to obtain a dataset with short temporal baselines that is needed for the STBAS method, is ordering and acquiring consecutive repeat pass observations. In this study we use Radarsat-1 observations with 24-day repeat pass interval, acquired over a two-year long period (2006–2008). The dataset is almost complete. It consists of 29 SAR images out of the 31 that were ordered. Thus most of the interferograms have 24-day temporal baseline (Table 2, Fig. 2). Unfortunately, two ordered images were not acquired, resulting in two interferograms with 48-day temporal baseline. The first 48-day interferometric pair shows enough coherent phase to provide useful information in our study (Fig. 5(1)). However, the other 48-day pair presents very low coherence in most of the study area (Fig. 5(17)). Consequently water level information derived from this interferogram is less accurate. In order to minimize the effect of this and other low coherent interferograms, we introduce a multiple calibration dates, which help in keeping the overall uncertainty (RMSE) level low.

In order to tie the relative InSAR observations with actual water levels, we used stage information in two calibration steps. In the first step, we calculated the offset between the InSAR and stage data to obtain actual water level changes. In the second step we tied the calibrated water level changes to a reference surface to obtain absolute water levels. When only one reference site is available, this site serves as the reference height point. When two or more reference sites are available, we use a least square fit to calculate deviation between InSAR and stage data. Theoretically the water level estimation accuracy (RMSE) should increase with the number of stations used in the calibrations. However in reality, the RMSE results can be degraded if additional stations are located in low coherence area, or too close to hydraulic structures. Although it is tempting to use stage data as is (raw data), the data should be used cautiously. In our study area, WCA-1, some of the stations are located near flow structures (gates) and are affected by the flow dynamics, consequently these stations can provide inaccurate stage values (Lin & Gregg, 1988). Thus, the stage data require editing prior to be used in the STBAS algorithm.

The actual comparison between InSAR and stage observations requires sometimes an innovative approach. In the simple case of the interior stations, a stage point measurement is compared with an average value calculated from 3×3 pixel window surrounding the station location. However stations located along the peripheral canals are also located very close (10–20 m) to levees and often to open water areas, where the interferometric coherence is low. Because the InSAR pixel size (roughly 50 m long/wide) the InSAR value cannot be calculated from the nine pixels surrounding the station, but from a similar size area with a shifted location towards the wetland interior. A simple shift to the nearest non-levee pixels seems a straightforward solution, but results in low quality InSAR observations due to the low interferometric coherence of the canal and large open water areas surrounding some of the stations (Fig. 6). In order to overcome the low coherence problem, we defined virtual stage stations located in areas of high coherence at the vicinity of each peripheral stage station (see Electronic Supplement). Before we implemented virtual stations selection procedure, the RMSE was in the range of 16–18 cm. Implementing the virtual station analysis improved significantly the quality of the STBAS analysis, as indicated by a much lower RMSE, in the range of 6–7 cm.

Transforming the relative InSAR measurements to absolute water levels requires a definition of reference water levels. We chose to use the almost flat water conditions at the end of the wet season (December–January) as the reference water level for the analysis. The STBAS algorism basically tracks absolute levels for each acquisition date, by adding or subtracting the InSAR-derived water level changes from the previous known level, starting with the reference level. Because the procedure is sequential, errors accumulate with time from the date of the reference level. In order to minimize the total error, which looks as a drift, we introduce multiple reference levels at the end of each wet season. Our results show that the selection of multiple calibration reference levels is very useful to obtain better results, especially when incoherent interferograms introduce large errors.

The uncertainty in determining absolute water levels is based on the total RMSE estimate, which is in the range of 6-7 cm (Table 4). These values reflect two major contributions: uncertainties in determining water level changes from the interferograms and

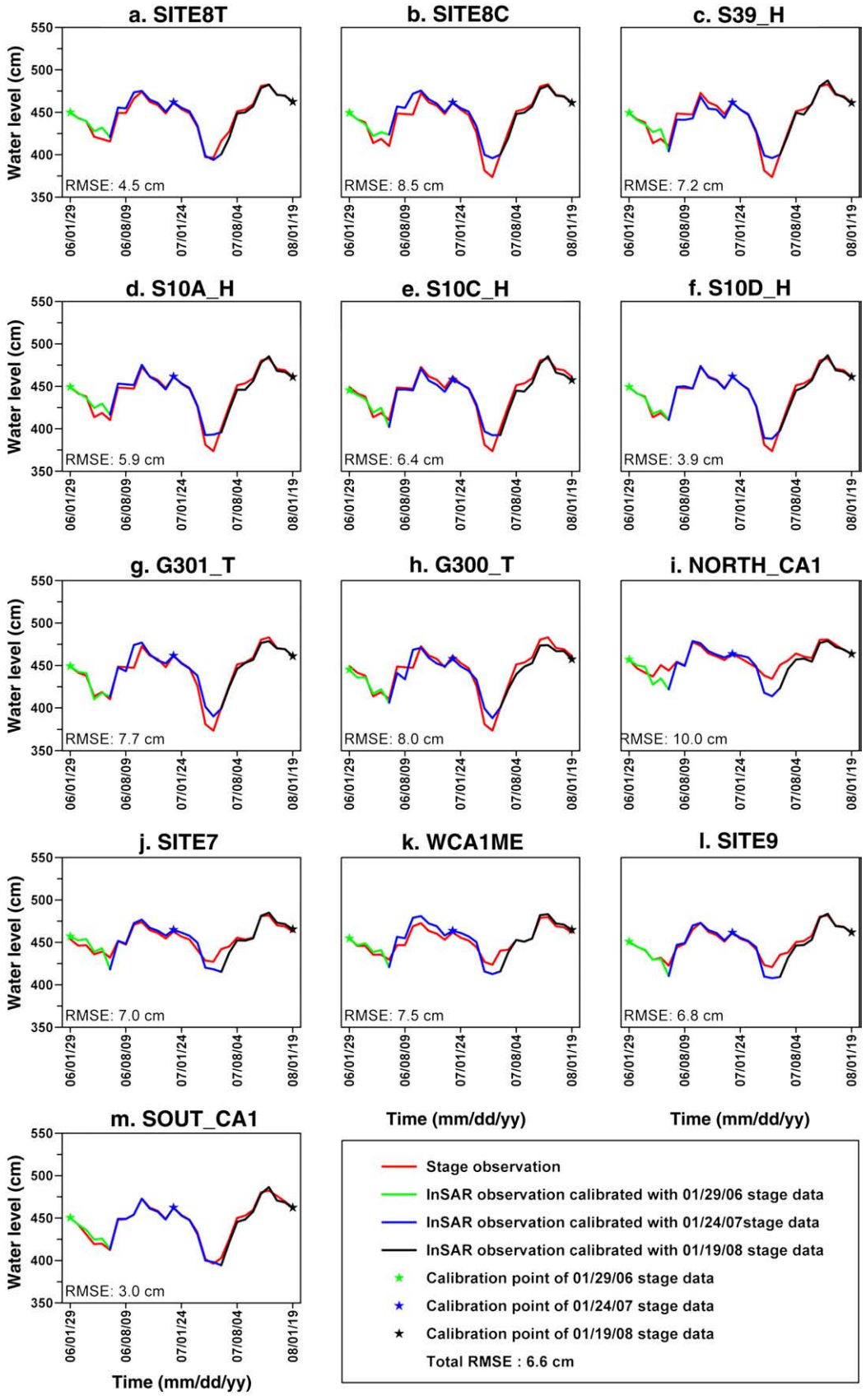

Fig. 10. Comparison between stage (red) and InSAR (green, blue and blank) determined water level time series. The graphs show good agreement between InSAR and stage station measurement. The InSAR series is based on test ID. 1 in Table 4.

uncertainties associated in the transition to absolute water levels. The virtual station analysis shows that the RMSE in determining relative water level changes is 3-4 cm (Table ES2-1). This uncertainty level probably reflects contributions from atmospheric noise, stage station data problems, and low coherence. An atmospheric delay variations in the troposphere can cause problems in interferogram interpretations (Hanssen, 2001). Unfortunately, atmospheric contribution phase, which is well estimated by the PSI and the SBAS techniques for solid surface applications, cannot be removed by the STBAS method in wetlands application, because it has a similar wavelength as fluctuating water level changes and, hence, is not sufficiently distinct. Thus the final water level time series probably contains some degree of the atmospheric noise. Another error source is low coherent observations, especially when the temporal baseline is 48 days. Finally, some errors can also be attributed to the stage measurements, which are affected by flow conditions (Lin & Gregg, 1988) and other possible disturbances. As part of our analysis, we edited the peripheral canal stage data. However, some additional errors can still embedded in the stage dataset. The difference between the total RMSE (6-7 cm) and the virtual station analysis (3-4 cm) reflects uncertainties associated with the transition from water level changes to absolute levels. The uncertainty difference is 4-5 cm, because it is calculated from variance and not directly from the RMSE values. This uncertainty most likely reflects deviation from the assumed flat water level condition used in the final calibration step 5.

The STBAS technique provides very high spatial resolution water level maps that cannot be obtained by any other terrestrial or space technique. Our analysis of WCA1 is based on the Radarsat-1 Fine beam (F5) observations acquired with 7 m pixel resolution. In order to increase the measurement signal, we applied a filtering technique, which degrades the spatial resolution to about 50 m. This degraded resolution is still an order of magnitude better than observations acquired by other techniques. Radar altimetry can measure water level height over rivers, lakes, and wetlands with 100-200 m footprint; however, the measurements acquire only along the satellite tracks, which are separated by more than 50-100 km from one another. The NASA/CNES planned Surface Water and Ocean Topography (SWOT) mission is based on a wide-swath altimetry technology with complete coverage of the world's oceans and freshwater bodies. Due to the wide swath, SWOT resolution is rather coarse, 100 m over rivers and 1000 m over lakes, reservoirs and wetlands. The current 50 m spatial resolution can be improved by the new generation of SAR satellites (TerraSAR-X, COSMO-Skymed) that can acquire data with a meter or sub-meter resolution. These data can be used to generate, after filtering, very high-resolution (10 m or less) final product of water level maps.

The high spatial resolution water level maps generated by the STBAS technique enable us to evaluate the quality of other such maps derived from stage data interpolation, in particular maps generated by the EDEN project (Conrads & Roehl, 2006; Pearlstine et al., 2008). The ground-based surface maps generated by EDEN are calculated using spatially continuous interpolation method with limited numbers of stage stations. In contrast, our space-based water surface maps are composed of real observed values in each pixel. Another difference between the STBAS and the EDEN maps is the spatial resolution, which is 50 m for the space-based observations and 400 m in the interpolated solution. Here we demonstrate the usefulness of the space-based observations that is characterized by a 50 cm level change across WCA-1 (Fig. 9). The comparison shows similar water level height variations in the range of 430-480 cm, but with very different distributions. The space-based map shows high water levels in the northeastern quadrant (Fig. 11a), whereas the interpolation-based map shows high level throughout the northern half of WCA-1 (Fig. 11b). Other differences also appear in the southern section of the study area. Based on the two maps, we calculated a residual map (Fig. 11c) showing a truncated pattern resulted from limited stage station points in the statistical interpolation processing. Significant differences between the two maps were found in areas located farthest from the stage stations. The major drawback of the space-based maps is its low temporal resolution. The Radatsat-1 dataset allow us to produce such maps once every 24 days. However, future satellite constellation missions, e.g., the Italian COSMO-Skymed, can provide observations every few days, which can significantly improve the temporal resolution of the space-based observations.

Our STBAS technique has a potential to be applied to other wetlands or relatively rapid changing surfaces such like ice sheets. The essential parameter for the implementation of the STBAS method is successive acquisitions of images with high coherence. In general, shorter temporal baseline provides better coherent interferometric phases (Hong & Won, 2006). Hence other space-borne sensors, such as TerraSAR-X with 11 days temporal baselines or COSMO-Skymed satellite constellation with 1-16 days temporal baselines, can be

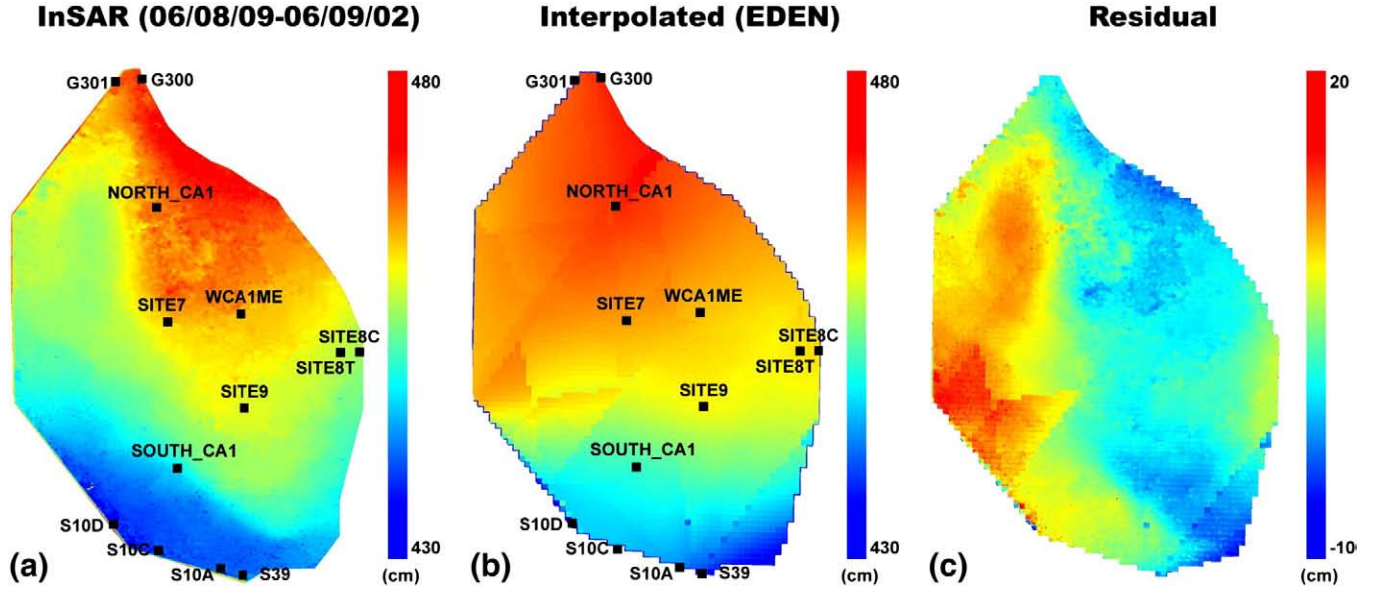

Fig. 11. Comparison between an InSAR observed surface (a) and an interpolated water surface (b). The interpolated surface is obtained from the EDEN daily averaged stage data. Residual map (c) shows deviation of up to 20 cm, indicating that the interpolated surface is limited in describing small wavelength variation mainly in the western side of WCA1.

useful for water level monitoring over wetlands using the STBAS method.

High spatial resolution maps of absolute water levels can serve as important constraints for wetland surface flow modeling. Wdowinski et al. (2004) showed that a subset of L-band InSAR observation are capable constraining a flow model and improve estimation of surface flow parameters. The hydrology of WCA1 was modeled by Meselhe et al. (2006), as a part of a water management tool. We believe that the space-based high spatial resolution observations can significantly improve the hydrological modeling of WCA1 and, hence, improve water management that depends on Meselhe's flow model.

7. Conclusions

We developed the STBAS method, which utilizes highly coherent interferometric phases obtained only with short time difference between two SAR acquisitions, for wetland InSAR application. The STBAS technique can transform relative wetland InSAR observations to absolute frame and generates both detailed maps of water levels, as well as water level time series for almost each pixel (50 m resolution). Both products are very useful to understand wetland surface flow patterns and manage wetlands efficiently. Although our study is limited to WCA1 located in the northern extent of the Everglades wetlands in south Florida, it has the potential to be used in other wetlands or other relatively rapid changing surfaces such like icesheets.

Using a RMSE analysis, we estimated the uncertainty of the STBAS algorithm for estimating absolute water levels as 6-7 cm. The individual station RSME varies in the range of 3-11 cm. The 6.6 cm uncertainty level reflects the sum of two major contributions. The first contribution is uncertainty of the InSAR measurement in detecting water level change, which is 3-4 cm based on our rigorous virtual station analysis. The additional uncertainty of 4-5 cm reflects error propagation due to the conversion from relative to absolute water levels. In order to allow an easy access to the InSAR multi-temporal data, we developed a STBAS tool for interactive display of water level maps, time series and water level points. It is a very useful tool for research and management purposes.

Acknowledgements

We thank Timothy Dixon for useful discussions and comments. This work is funded through NASA Cooperative Agreement No. NNX08BA43A (WaterSCAPES: Science of Coupled Aquatic Processes in Ecosystems from Space) grants. We thank CSA for access to the Radarsat-1 data, JAXA for access to Jers-1 data, SFWMD and USGS for access to stage data. This is CSTARS contribution No. 26.

Appendix A. Supplementary data

Supplementary data associated with this article can be found, in the online version, at doi:10.1016/j.rse.2010.05.019.

References

Alsdorf, D. E., Melack, J. M., Dunne, T., Mertes, L. A. K., Hess, L. L., & Smith, L. C. (2000). Interferometric radar measurements of water level changes on the Amazon flood plain. *Nature*, *404*, 174—177.

Berardino, P., Fornaro, G., Lanari, R., & Sansosti, E. (2002). A new algorithm for surface deformation monitoring based on small baseline differential SAR interferograms. *IEEE Transactions on Geoscience and Remote Sensing*, *40*, 2375—2383.

Buckley, S.M., Rossen, P.A., & Persaud, P. (2000). ROI_PAC documentation — Repeat orbit interferometry package.

Conrads, P. A., & Roehl, E. A. (2006). Estimating water depths using artificial neural networks. *Hydroinformatics*, *2006*(3), 1643—1650.

Ferretti, A., Prati, C., & Rocca, F. (2000). Nonlinear subsidence rate estimation using permanent scatterers in differential SAR interferometry. *IEEE Transactions on Geoscience and Remote Sensing*, *38*, 2202—2212.

Ferretti, A., Prati, C., & Rocca, F. (2001). Permanent scatterers in SAR interferometry. *IEEE Transactions on Geoscience and Remote Sensing*, *39*, 8—20.

Goldstein, R. M., & Werner, C. L. (1998). Radar interferogram filtering for geophysical applications. *Geophysical Research Letters*, *25*, 4035—4038.

Gondwe B. R. N., Hong S. -H., Wdowinski, S., & Bauer-Gottwein, P. (2010). Hydrodynamics of the groundwater-dependent Sian Ka'an wetlands, Mexico, from InSAR and SAR data, Wetlands, 30, 1–13.

Hanssen, R. (2001). Radar interferometry: Data interpretation and error analysis. Kluwer Academic Publishers.

Hong, S. -H., Wdowinski, S., & Kim, S. -W. (2010). Evaluation of TerraSAR-X observations for wetland InSAR application. *IEEE Transactions on Geoscience and Remote Sensing*, *48*, 864—873.

Hong, S. H., & Won, J. S. (2006). Application of ERS-ENVISAT cross-interferometry to coastal DEM construction. *Proceedings of EUSAR'06, Dresden, Germany, 16–18, May*.

Kim, S. -W., Wdowinski, S., Amelung, F., Dixon, T., & Hong, S. -H. (2008). X-band InSAR Observations in New Orleans, Louisiana. *IGARSS 2008: Boston, U.S.A*.

Kim, S.-W., Wdowinski, S., Amelung, F., Dixon, T., & Won, J.-S. submitted for publication. Interferometric coherence analysis of the Everglades wetlands, South Florida. *IEEE Transactions on Geoscience and Remote Sensing.*

Lanari, R., Mora, O., Manunta, M., Mallorqui, J. J., Berardino, P., & Sansosti, E. (2004). A small-baseline approach for investigating deformations on full-resolution differential SAR interferograms. *IEEE Transactions on Geoscience and Remote Sensing*, *42*, 1377—1386.

Lin, S., & Gregg, R. (1988). Water budget analysis water conservation area 1. DRE 245, June.

Lu, Z., Crane, M., Kwoun, O., Wells, C., Swarzenski, C., & Rykhus, R. (2005). C-band radar observes water level change in swamp forests. *EOS, Transactions, AGU*, *86*, 141—144.

Lu, Z., & Kwoun, O. I. (2008). Radarsat-1 and ERS InSAR analysis over southeastern coastal Louisiana: Implications for mapping water-level changes beneath swamp forests. *IEEE Transactions on Geoscience and Remote Sensing*, *46*, 2167—2184.

Meselhe, E. A., Griborio, A., & Arceneaux, J. (2006). Model selection report. *Report #LOXA05-001, June*.

Mitsch, W. J., & Gosselink, J. G. (2007). *Wetlands.* New Jersey: John Wiley & Sons, Inc.

Pearlstine, L., Palaseanu-Lovejoy, M., Telis, P., Henkel, H., & Higer, A. (2008). Spatially continuous interpolation of water stage and water depths using the Everglades depth estimation network (EDEN). *USGS Modeling Conference, Orange Beach, Ala., February 11-15*.

Press, W. H., Teukolsky, S. A., Vetterling, W. T., & Flannery, B. P. (2002). Numerical recipes in C: the art of scientific computing. : Cambridge Cambridge Univ. Press.

Richards, J. A., Woodgate, P. W., & Skidmore, A. K. (1987). An explanation of enhanced radar backscattering from flooded forests. *International Journal of Remote Sensing*, *8*, 1093—1100.

Rivera, S. (2005). *Wetland.* Minneapolis: Lerner Publications Company.

Wdowinski, S., Amelung, F., Miralles-Wilhelm, F., Dixon, T. H., & Carande, R. (2004). Space-based measurements of sheet-flow characteristics in the Everglades wetland, Florida. *Geophysical Research Letters*, *31*.

Wdowinski, S., Kim, S. W., Amelung, F., Dixon, T. H., Miralles-Wilhelm, F., & Sonenshein, R. (2008). Space-based detection of wetlands' surface water level changes from L-band SAR interferometry. *Remote Sensing of Environment*, *112*, 681—696.

Wdowinski, S., S.-W., K., Amelung, F., & Dixon, T. (2006). Wetland InSAR: A new space-based hydrological monitoring tool of wetlands surface water level changes. *GlobWetland symposium proceedings*.